applied sciences

MDPI

Article

Thermo-Mechanical Properties of PLA/Short Flax Fiber Biocomposites

Laura Aliotta *, Vito Gigante, Maria-Beatrice Coltelli, Patrizia Cinelli, Andrea Lazzeri and Maurizia Seggiani *

Department of Civil and Industrial Engineering, University of Pisa, 56122 Pisa, Italy

* Correspondence: laura.aliotta@dici.unipi.it (L.A.); maurizia.seggiani@unipi.it (M.S.); Tel.: +39-05-0221-7854 (L.A.); +39-05-0221-7881 (M.S.)

Received: 7 August 2019; Accepted: 6 September 2019; Published: 11 September 2019

Abstract: In this work, biocomposites based on poly(lactic acid) (PLA) and short flax fibers (10–40 wt.%) were produced by extrusion and characterized in terms of thermal, mechanical, morphological, and thermo-mechanical properties. Analytical models were adopted to predict the tensile properties (stress at break and elastic modulus) of the composites, and to assess the matrix/fiber interface adhesion. The resulting composites were easily processable by extrusion and injection molding up to 40 wt.% of flax fibers. It was observed that despite any superficial treatment of fibers, the matrix/fiber adhesion was found to be sufficiently strong to ensure an efficient load transfer between the two components obtaining composites with good mechanical properties. The best mechanical performance, in terms of break stress (66 MPa), was obtained with 20 wt.% of flax fibers. The flax fiber acted also as nucleating agent for PLA, leading to an increment of the composite stiffness and, at 40 wt.% of flax fibers, improving the elastic modulus decay near the PLA glass transition temperature.

Keywords: poly(lactic acid); flax fibers; biocomposites; predictive analytical model; mechanical properties

1. Introduction

The development of biocomposites, produced using a biopolymer matrix and a reinforcement from renewable resources, is currently an extensive research area due to the promising mechanical properties, recyclability after service [1], and biodegradability [2] of these materials. These composites have potential applications in different fields such as automotive, packaging, and household goods [3]. Clearly, the application of natural fibers is being driven not only by environmental reasons, but also by economical ones. Natural fiber-reinforced composites, in fact, can be used as low-cost materials having at the same time different structural properties [4].

The use of natural fibers has many advantages. Natural fibers are renewable, biodegradable, and less abrasive to tooling. Furthermore, they can be formed into light composites leading to weight reductions and, especially in automotive field, to fuel saving [5]. Among natural fibers, lignocellulosic fibers are investigated as promising substitutes of the synthetic fibers in polymeric composites and several studies have examined drawbacks and advantages of the most significant lignocellulosic fibers and their related polymeric composites [6–9].

One of the strongest natural fibers is the flax fiber. Their structure is very complex and can be compared to a composite structure. In fact, the flax fibers are constituted by a series of polyhedron shape elementary fibers overlapped over a considerable length; they are held together by an interphase that mainly consists of hemicellulose and pectin. Each elementary fiber consists of a very thin primary cell wall, a secondary cell wall (dominating the cross section), and an open channel at the fiber center called "lumen" [10–12]. Typical dimeter for an elementary flax fibers are around 10–15 μm; on the other hand, technical flax fibers have a diameter that varies between 35–150 μm [11].

Different biopolymers such as poly(lactic acid) (PLA), polyhydroxyalkanoates (PHAs), and cellulose esters have been used as matrices coupled with natural fibers for various applications [13–15]. Among these biopolymers, PLA is currently one of the most used and promising biopolymers because of its lower production cost compared to that of other biopolymers such as PHAs, poly-butylene succinate (PBS), poly-butylene succinate-*co*-adipate (PBSA). PLA exhibits, at room temperature, very good mechanical properties: Young modulus of 3 GPa, tensile strength between 50 and 70 MPa, and impact resistance of 2.5–3 kJ/m^2 [16,17]. However, PLA is very stiff and brittle with poor thermal properties and a very slow crystallization rate; often it is necessary to use a plasticizer or introduce rubber particles to improve its break elongation and impact properties [18–20], while nucleating agents are added to increase its crystallinity and enhance its thermal stability [21].

Some of PLA drawbacks may be overcome by fiber-reinforcement and blending. Mechanical properties of natural fiber-reinforced PLA composites have been investigated by different researchers and different types of natural fibers were used in place of synthetic fibers [22]. However, the addition of natural fibers to polymeric matrices requires special attention in order to obtain biocomposites with good mechanical properties. In fact, compared to the synthetic composites, the composites containing natural fibers generally show lower mechanical properties, higher moisture absorption, and lower durability [23]. Many researchers have been working to address these issues, with particular attention to the surface treatments of the natural fibers and the improvement of the fiber/matrix adhesion. In fact, the fiber/matrix adhesion plays an important role in the final mechanical properties of the composites since a good adhesion guarantees an efficient transfer of the stress between the matrix and the fiber, obtaining the desired reinforcement. Natural fibers, containing a large amount of cellulose, hemicellulose, lignin, and pectin, tend to be active polar hydrophilic material while polymer matrices are not polar and exhibit hydrophobic properties. So there is typically a weak interfacial bonding between the highly polar natural fiber and non-polar organophilic matrix and this leads to a loss of the mechanical properties of the resultant composites [24]. Different approaches have been investigated to improve the interfacial compatibility and bond strength as the use of surface modification techniques [4,25]. The strength of the interfacial bond depends on different parameters as surface energy, chemistry, and fiber roughness that can be modified by different treatments [26,27]. In particular, chemical treatments with sodium hydroxide, peroxides, organic, and inorganic acids, silane, anhydrides, and acrylic monomers have been proposed to remove non-cellulosic components (in cellulosic fibers) and to add functional groups that provides better chemical bonding between the treated fibers and the polymeric matrix [28]. A weak interface adhesion decreases the composite tensile strength but increases the impact resistance, due to the fiber pull-out mechanism. On the other hand, a strong interface adhesion generally leads to a stiff composite having high tensile strength but brittle impact behavior (fiber pull-out is prevented) [29].

The fabrication methods of composites based on PLA and natural fiber such as flax fibers are the same as those used for the thermoplastics in which short fibers are added and traditional molding methods such as extrusion, compression, and injection molding are used [22]. The adopted processing conditions (screw speed, profile temperature, pressure, residence time, etc.) influence the final mechanical properties of PLA/fiber composites. The fibers damaging due to the long permanence at high temperature or to an excessive screw speed must to be considered. In particular, it was observed that compression molding technique does not damage the natural fiber during processing. However, this technique is time consuming and unsuitable for mass production. On the contrary, for high productions, the injection molding is used, showing easy processability that allows the prevention of fiber degradation during the process and generally it improves the fiber dispersion in the matrix [23]. In terms of fiber length, compression and hot press molding can be used for both long and short fibers, while injection molding can process only short fibers. Oksman et al. [30] manufactured PLA/flax fiber composites with a twin-screw extruder up to 40 wt.% of long fibers, followed by compression molding. Bax and Müssig [31] have produced PLA/flax fiber composites up to 30 wt.% fibers, using hot-pressing followed by pelletizing and injection molding.

In the present study, biocomposites based on PLA containing un-treated short flax fibers, up to 40 wt.% of fibers, were produced by melt extrusion followed by injection molding. The developed composites were characterized in terms of tensile properties, thermal properties by differential scanning calorimetry (DSC), and thermo-mechanical properties by dynamic mechanical thermal analysis (DMTA). Scanning electron microscopy (SEM) analysis was carried out to evaluate the fiber/matrix interface and the dispersion/structure of the fibers in the PLA matrix. Analytical models were used to predict the tensile properties of the developed composites and to assess the interfacial matrix/fiber adhesion.

2. Materials and Methods

2.1. Materials

PLA used in this study was PLA 2003D from NatureWorks LLC (Minnetonka, MN, USA), grade for thermoforming and extrusion processes with melt flow index (MFI) of 6 g/10 min (210 °C, 2.16 kg), having a nominal average molar mass of 200,000 g/mol, density of 1.24 g/cm^3, content of D-lactic acid units of 3–6%).

Chopped flax fibers with average length of 1 mm and aspect ratio of 8 were used as natural fibers. To evaluate the fiber volume fraction in the composites a density of 1.5 g/cm^3 [12] was considered.

2.2. Composite Preparation

All materials were dried in a circulating air oven at 60 °C for at least 24 h before the composite preparation. Formulations with 10, 20, and 40 wt % flax fibres, with respect to the total weight, were produced by melt blending using a Thermo Scientific™ HAAKE™ MiniLab II micro-compounder, a co-rotating conical twin-screw extruder with a screw rate of 110 rpm/min, a cycle time of 60 s at 180 °C; at this temperature PLA is at the molten state and the flax fibers are thermally stable. Sample names with the relative compositions in weight and volume are reported in Table 1.

Table 1. Composites and relative compositions.

Sample	PLA/Fiber (wt./wt.%/%)	PLA/Fiber (vol./vol.%/%)
PLA	100/0	100/0
PF10	90/10	92/8
PF20	80/20	83/17
PF40	60/40	64/36

After extrusion, the molten material was transferred, through a preheated cylinder, to a Thermo Scientific Haake MiniJet II mini injection press (mold temperature set at 70 °C) for the production of Haake type III dog-bone tensile specimens (size: 25 × 5 × 1.5 mm). The injection molding was carried out at 180 °C, at pressure of 680 bar and with a residence time in the mold of 15 s for all the tested formulations. In fact, as observed by Bos et al. [10], the thermal degradation of flax fibers starts at around 200 °C and it is not significant in the first minutes. Before thermal and mechanical tests, the specimens were stored in a climate chamber at room temperature and controlled relative humidity of 50%.

2.3. Tensile Tests

Tensile tests were carried out at room temperature and at a crosshead speed of 10 mm/min by an Instron 5500 R universal testing machine (Canton, MA, USA) equipped with a 10 kN load cell and interfaced with a computer running MERLIN software (version 4.42S/N-014733H). The samples were tested after 24 h from injection molding process. At least five specimens for each composite were tested and the average values were reported.

2.4. Morphological Analysis

The flax fibers and the cryogenic facturated cross-sections of the composites were analyzed by SEM (JEOL JSM-5600LV, Tokyo, Japan). In addition, SEM analysis was carried out also on the fractured sections of the dog-bone specimens obtained after doing tensile tests in order to evaluate the fiber-matrix adhesion. Prior to the morphological analysis, all the samples were coated with a gold layer.

2.5. Calorimetric Analysis

The composite sample used for the DSC analysis was obtained by cutting the corresponding tensile specimen and about 10–15 mg of sample was placed in sealed aluminum pan. The eventual crystallization of PLA that can occur during the injection molding process was evaluated using the first heating run from 25 to 200 °C at 10 °C/min. On the other hand, the second heating was also performed to eliminate the thermal history of the sample. After the first heating, the material was kept at 200 °C for 5 min to ensure the complete melting of the crystals and, then, it was cooled at 10 °C/min from 200 to 40 °C. Finally, the second heating was performed at 10 °C/min from 40 to 200 °C.

The cold crystallization temperature (T_{cc}) and the melting temperature (T_m) were evaluated in correspondence of the minimum cold crystallization peak and the maximum melting peak, respectively. Whereas, the enthalpies of cold crystallization (ΔH_{cc}) and melting (ΔH_m) were calculated as the areas of the corresponding peaks.

The degree of crystallinity (X_{cc}) of pure *PLA* and composites was determined using the following equation:

$$X_{cc} = \frac{\Delta H_m - \Delta H_{cc}}{\frac{\Delta H^{\circ}_m}{wt.\ \%\ of\ PLA}} \quad (1)$$

where $\Delta H^{\circ}{}_m$ is the theoretical melting heat of 100% crystalline *PLA*. Because of the materials were processed in the range of the disorder-to-order phase transition [32] a double peak, due to the existence of α′ and α crystalline phases, is present. As a consequence, considering the $\Delta H^{\circ}{}_m$ values of α′ and α phases [33], a mean value between the $\Delta H^{\circ}{}_m$ of α′ (107 J/g) and $\Delta H^{\circ}{}_m$ of α (143 J/g) was adopted (125 J/g) according to other studies [17].

2.6. Thermo-Mechanical Analysis

Dynamic mechanical thermal analysis (DMTA) was carried out using a Gabo Eplexor® DMTA (Gabo Qualimeter, Ahiden, Germany) with a 100N load cell. At least two specimens were tested for each composite. Test bars (size: 20 × 5 × 1.5 mm), obtained by cutting the tensile specimens, were mounted on the machine in tensile configuration. The used temperature range varied from 35 to 120 °C with heating rate of 1.5 °C/min and at a constant frequency of 1 Hz.

3. Predictive Models of Mechanical Properties

In this work, different analytical models were adopted to better understand the results of the mechanical tests and to predict the mechanical properties of the composites as function of the fiber content.

3.1. Break Strength Prediction

The break strength is strongly affected by the adhesion between the fibers and the matrix [34]. Different analytical models, based on modified Kelly–Tyson equation, were proposed to predict the interfacial shear stress (IFSS) of composite taking into account the properties of the fibers and the matrix [35–37]. However, to apply them, it is necessary to know the critical length and the length distribution of the fibers into the composite. Since the procedure to have an IFSS estimation is laborious,

one of the most used simple models to predict the yield/break strength and the fiber/matrix interaction is the Pukánszky's model [38,39] based on the Equation (2):

$$ln\sigma_{c,red} = ln\frac{\sigma_c\left(1+2.5V_f\right)}{\sigma_m\left(1-V_f\right)} = BV_f \quad (2)$$

where $\sigma_{c,red}$ is the predicted reduced stress (adimensional) of the composite that takes into account the reduced bearing section of the composites due to the presence of the filler, σ_c and σ_m are the stress at yield/break of the composite and matrix, respectively, V_f is the filler volume fraction, and B is the Pukánszky's interaction parameter. Plotting the natural logarithm of the reduced stress $\sigma_{c,red}$ as a function of V_f, the B parameter can be calculated from the slope of the linear correlation obtained. Consequently, applying the dependence of the strength on composition, an estimate of the fiber-matrix interaction can be obtained.

Although the B parameter has no a direct physical meaning, it is obviously connected with the interfacial properties of the system and it also depends on the matrix mechanical properties. The B parameter is related to the relative load-bearing capacity of the fiber, which depends by the interfacial interactions. The relationship between the B parameter and the interfacial properties is reported in the following equation (Equation (3)) [34]:

$$B = \left(1 + A_f\rho_f l\right)ln\frac{\sigma_i}{\sigma_m} \quad (3)$$

where A_f, ρ_f, l and σ_i are the specific filler surface area, the filler density, the thickness of the interface and the strength of the interface, respectively.

3.2. Elastic Modulus Prediction

The composites analyzed are constituted by short flax fibers randomly oriented in the PLA matrix. The analytical models for short fibers were derived from the elasticity theory, starting from the models developed for long fiber composites. To better fit the experimental data and to take into account the differences between long and short fiber composites, a consistent numbers of geometrical, topological, and mechanical parameters [6,34] must to be taken into account. Different efforts to fit analytical models with experimental data can be found [40].

However, due to the low aspect ratio, it can be expected that the mechanical behavior and the elastic response of the produced composites is similar to the behavior of particulate filled composites. Consequently, some analytical models suitable for particulate filled composites [41–43] were applied to the PLA/short flax fibers composites. The analytical models adopted in this work to predict the Young's modulus of the composites are reported in Table 2.

Table 2. Analytical models used for the prediction of the composite Young's modulus.

Model	E $_{composite}$
Einstein [43]	$E_c = E_m\left(1+2.5V_f\right)$
Van Dyck [42]	$E_c = E_m\left(1+\frac{1.25\cdot V_f}{1-1.2\cdot V_f}\right)$
Cox [40]	$E_c = \left(1-V_f\right)E_m + V_f E_f\cdot\left(1-\frac{\tan h(n\cdot a_r)}{(n\cdot a_r)}\right)$
Halpin-Tsai [44]	$E_c = \frac{3}{8}E_l + \frac{5}{8}E_t$

In the models of Table 2, E_c, E_m, and E_f represent the elastic modulus of the composite, matrix and fibers, respectively, V_f is the fiber volume fraction, a_r is the aspect ratio of the fibers. The adimensional parameter n of the Cox model is defined as (Equation (4)) [45]:

$$n = \frac{2E_m}{E_f(1+\upsilon)ln\left(\frac{P}{V_f}\right)} \tag{4}$$

where υ is the Poisson ratio of the matrix (≈0.4) and P is the packing factor of the fibers, considered equal to $2\pi/\sqrt{3}$.

Concerning the Halpin–Tsai model [44], the two terms E_l and E_t are, respectively, the longitudinal and the tangential modulus; these values can be calculated by the following equations:

$$E_l = E_m \cdot \frac{1 + 2 \cdot a_r \cdot \left(\frac{\frac{E_f}{E_m} - 1}{\frac{E_f}{E_m} + 2a_r} \right) \cdot V_f}{1 - \left(\frac{\frac{E_f}{E_m} - 1}{\frac{E_f}{E_m} + 2a_r} \right) \cdot V_f} \tag{5}$$

$$E_t = E_m \cdot \frac{1 + 2 \cdot a_r \cdot \left(\frac{\frac{E_f}{E_m} - 1}{\frac{E_f}{E_m} + 2} \right) \cdot V_f}{1 - \left(\frac{\frac{E_f}{E_m} - 1}{\frac{E_f}{E_m} + 2} \right) \cdot V_f} \tag{6}$$

4. Results and Discussion

4.1. Processability

The possibility to use conventional melt processes is a very important for industrial use of these bio-composites. In this case PLA/flax fiber composites did not show any difficulties during the extrusion followed by injection molding. Under the same operating conditions adopted for the extrusion and injection molding, the mold filling was always complete, obtaining well-formed specimens also with 40 wt.% of fibers. These results are in accordance with the findings of Oksman et al. [30] who did not experience any difficulties in the extrusion and compression molding processes of PLA/long flax fiber composites up to 40 wt.% fibers.

4.2. Mechanical Properties and Modeling

Figure 1 shows the typical stress-strain curves of the PLA/flax fiber composites. As shown, PLA and all the composites show a fragile break without yielding. The main tensile properties are summarized in Figure 2.

As expected, the stiffness increased with increasing amount of flax fibers. This behavior is very common to other similar bio-composite systems encountered in literature [6]. The stiffness increase was reflected in a decrease in elongation at break. The tensile strength slightly increased with the fiber content up to 20 wt.% of fibers and, then, at higher fiber loading it resulted similar to that of pure PLA. This trend can be attributed to the well-known reinforcement effect of the flax fibers [30] up to 20 wt.%, while at 40 wt.% poor wetting of the fibers with the matrix may be present leading to reduced stress transfer across the fiber–matrix interface with consequent reduction of the tensile strength.

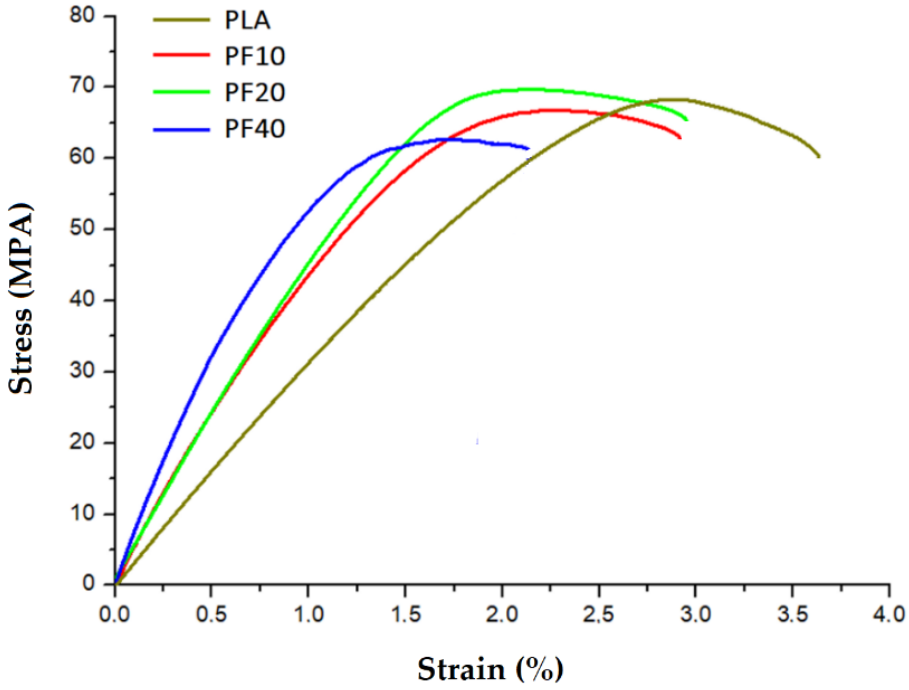

Figure 1. Stress-strain representative curves for pure poly(lactic acid) (PLA) and for PLA/flax fiber composites.

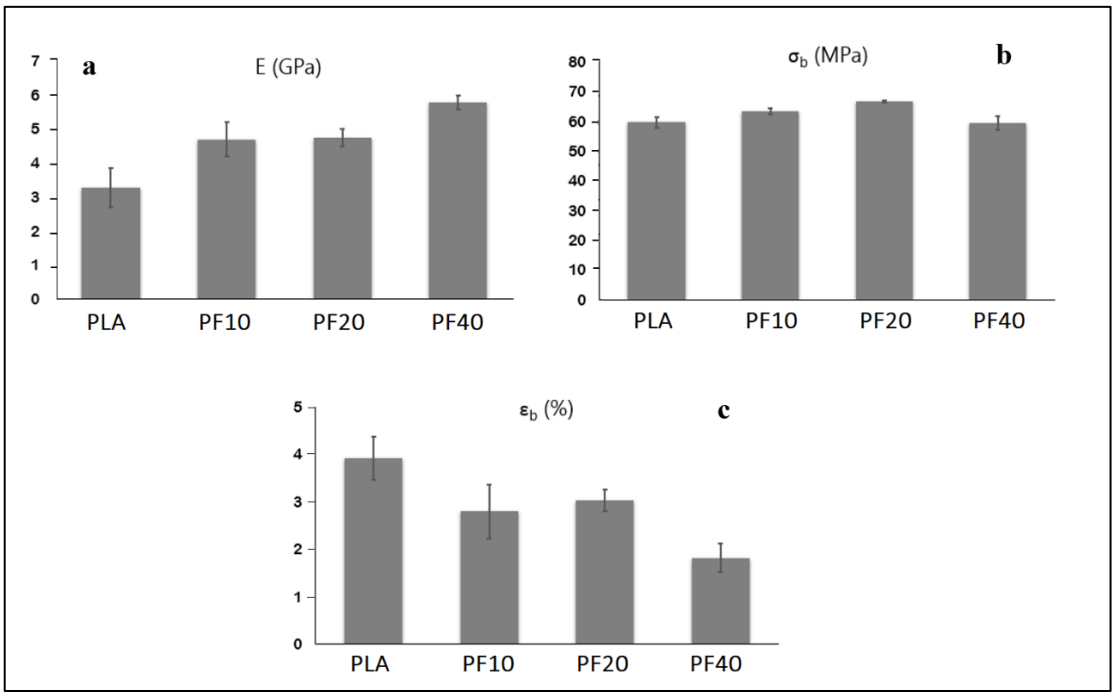

Figure 2. Mechanical properties for pure PLA and PLA/flax composites: (**a**) Elastic modulus; (**b**) Stress at break; (**c**) Elongation at break.

The values of the tensile strength are in agreement with those reported by Oksman et al. [30] and Bax and Müssig [31] that obtained tensile strengths of 53–54 MPa with 30 wt.% of fibers without fiber treatments and additives. In addition, the value for the Young's moduli of the PF20 is close to that found by Bax and Müssig [31] with 20 wt.% fibers (5.1 GPa).

Using the mechanical properties of the matrix (neat PLA) and the composites, the Pukánszky's plot can be obtained (Figure 3) and the B parameter can be evaluated.

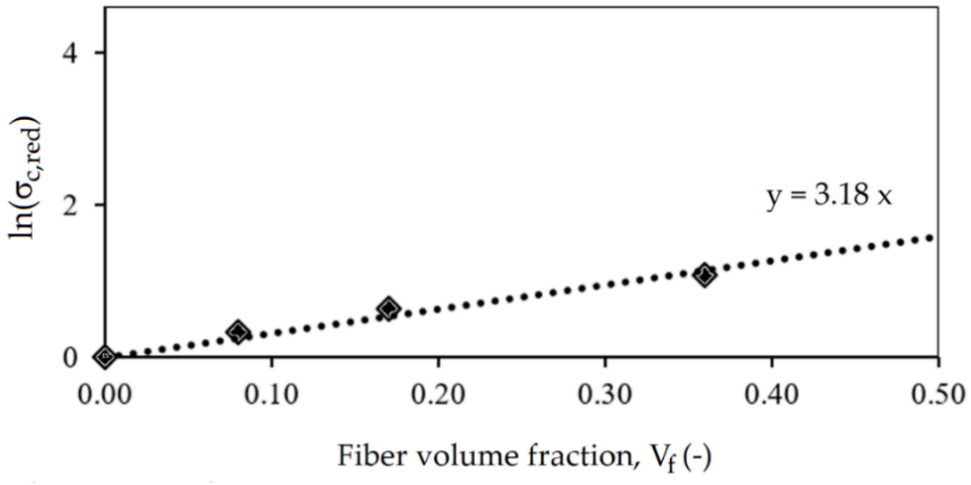

Figure 3. Pukánszky's plot for PLA/flax fiber composites.

The interaction B parameter value of about 3.2 indicates a good adhesion between the fibers and the matrix. In fact, in the case of weak interfacial bonding, the fibers do not carry the load and, consequently, B is almost zero [41]. This result is coherent with the general increase of the tensile strength of the composites indicating a good load transfer between the fibers and the matrix.

Interesting results were achieved using the analytical models for predicting the elastic modulus of the composites. In fact, as shown in Figure 4, the Cox and Halpin–Tsai models, typically used for aligned long fiber composites, did not fit the experimental data, especially at high fiber loading. On the other hand, the models for particulate filled systems (Einstein and Van Dyck models) provided a good fitting. This confirms that when the fibers are very short the mechanical behavior of their composites can be assimilated, as expected, to that of the particulate filled composites.

Furthermore, it can be confirmed the good adhesion between the fibers and the matrix since the Einstein model presupposes a perfect adhesion between the filler and the matrix and a good filler dispersion [46].

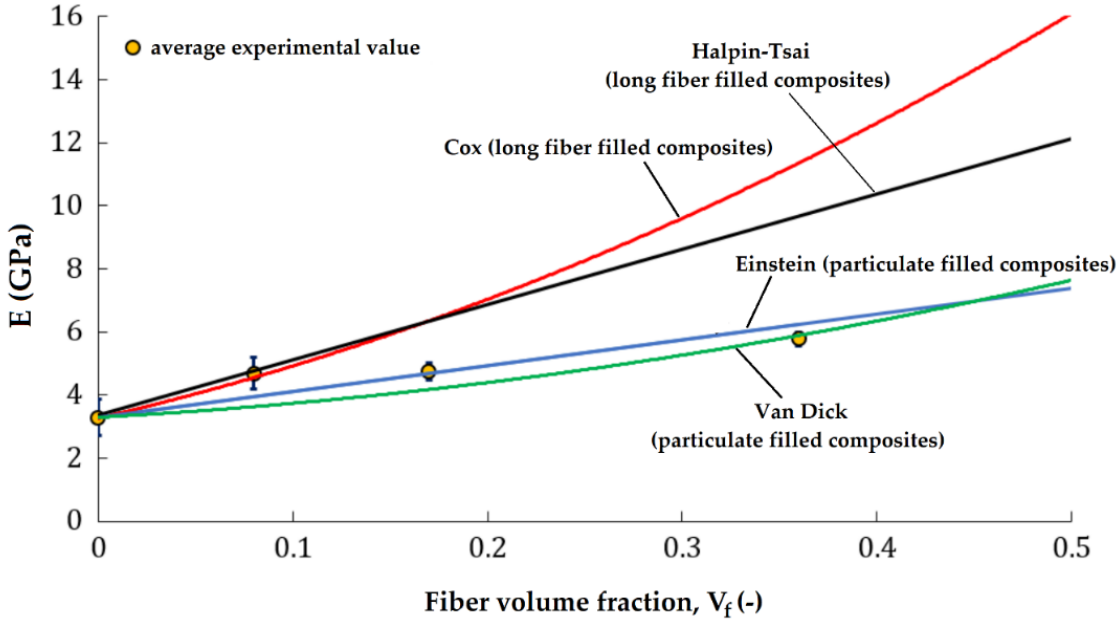

Figure 4. Comparison between experimental elastic modulus of the PLA/flax fiber composites and some predictive analytical models.

4.3. Morphological Analysis

SEM images of the chopped flax fibers and, as an example, the cross-sections of the composite with 10 wt.% flax fibers are reported in Figures 5 and 6, respectively. Further, Figure 7 shows the broken sections of the dog-bone specimens at different fiber loadings after doing tensile test.

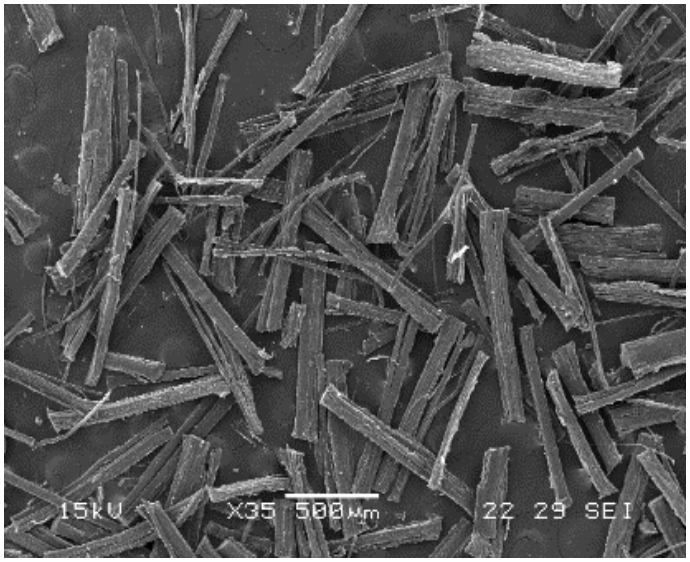

Figure 5. Chopped flax fibers used in this work.

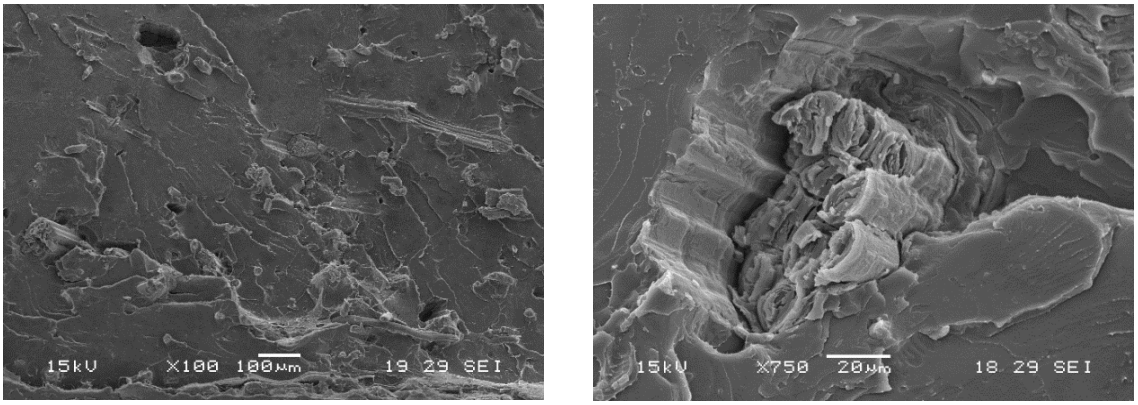

(**a**) (**b**)

Figure 6. SEM images of PLA/flax fibers composites with 10 wt.% flax fibers at (**a**) ×100 and (**b**) ×750 magnification.

It can be noticed that, due to their very low aspect ratio, no twisting was observed; however, a slight damage, due to the extrusion process, can be observed as many fibers became thinner and weaker.

As shown, the short flax fibers show a straight shape and appear like sticks. Figure 6b shows the typical polyhedron shape of flax fibers in which the elementary fibers are held pack together; the interphase is constituted by hemicellulose and pectin [5]. The adhesion between the fibers and the matrix is good; the fibers appear well adherent to the matrix and the very small space between the matrix and the fibers can be attributable to the different contraction/expansion coefficient of the fiber and matrix during the cryogenic fracture (Figure 6b). This supports the results of mechanical tests and analytical modelling. This good adhesion is confirmed also by the Figure 7 where there are many fibers that remain adhered to the matrix under the traction action and a moderate pull-out is observed. In addition, observing Figure 7, the short fibers are randomly oriented within the matrix and maintain their original straight shape without incurring evident deformation during the extrusion process.

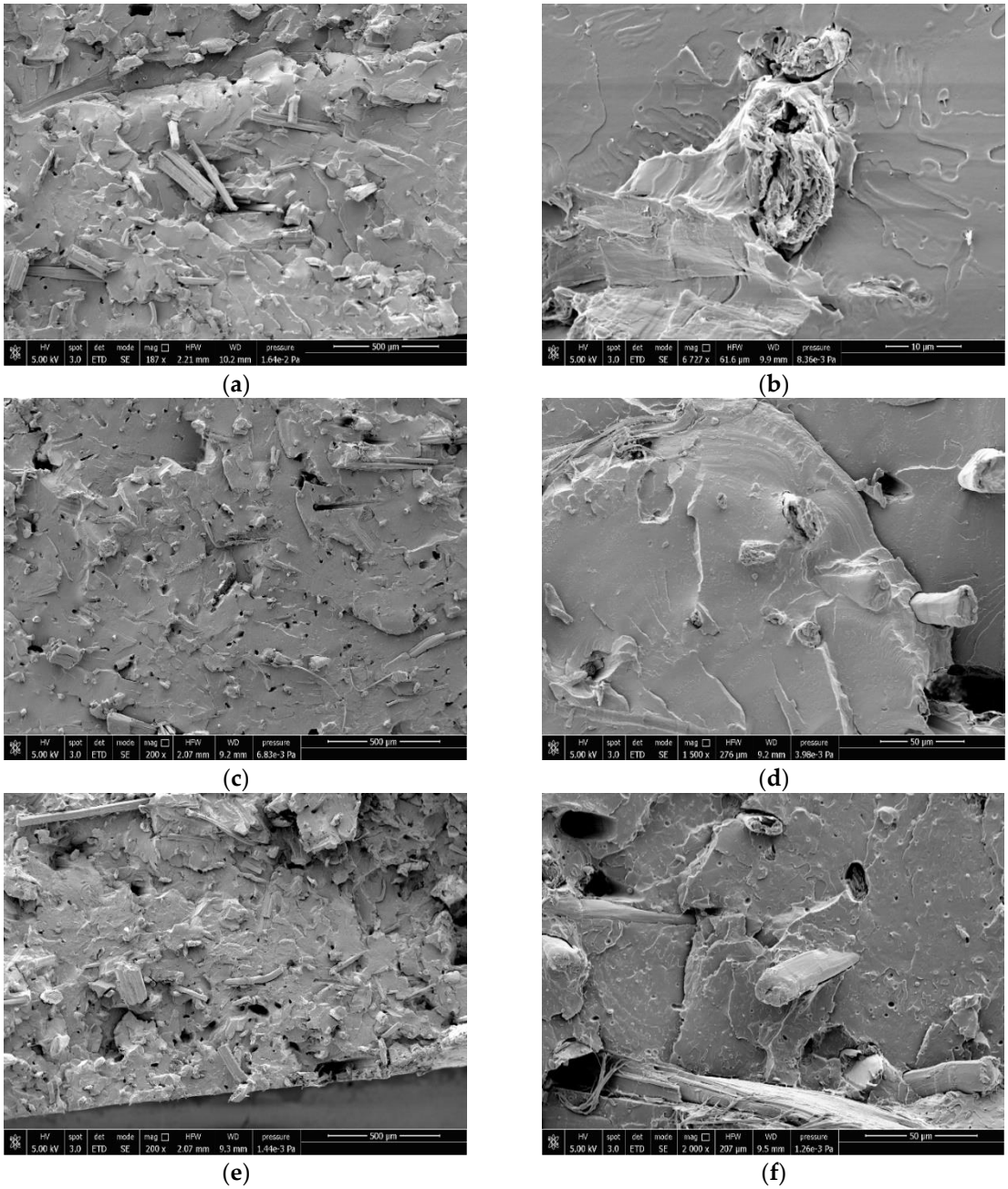

Figure 7. SEM images, at different magnifications, of PLA/flax fibers composites: (**a**,**b**) 10 wt.% of flax fibers, (**c**,**d**) 20 wt.% of flax fibers and (**e**,**f**) 40 wt. % of flax fibers.

Few works on the adhesion between PLA and flax fibers in biocomposites have been published. Most publications on the flax fiber composites concern the interaction between flax fibers and polymers including polypropylene (PP), polystyrene (PS), epoxy, bio-epoxy, and bio-phenolic resin, epoxy resins [47,48]. It is known that natural fibers have a poor adhesion to hydrophobic matrices like PP, because of their hydrophilic nature; consequently, to improve the interaction between these hydrophobic matrices and the flax fibers several chemical treatments were proposed such as mercerization, silane treatment, acylation, peroxide treatment and coatings [47,49,50]. Whereas, because of the hydrophilic nature of PLA a better interaction between PLA and flax fibers than between PP or epoxy resins and flax fibers can be expected as assumed by Heinemann and Fritz [51]. Nevertheless, Oksman et al. [30] and Bax and Müssig [31] observed a poor adhesion between long un-treated flax fibers and the PLA

matrix and they concluded that adhesion needs to be improved to optimize the mechanical properties of the PLA/flax composites. In this case, very short flax fibers were used and the good adhesion, evidenced by SEM analyses and the analytical modelling, between the short un-treated flax fibers and the PLA matrix can be attributable to the short length of the fibers (low aspect ratio) which facilitated the dispersion of the fibers within the matrix and reduced the fiber agglomeration favoring the wetting of all the fibers by the matrix.

4.4. Calorimetric Analysis

Figure 8 shows the DSC thermograms of first and second heating run for neat PLA and its composites. The resultant thermal properties (T_g, T_{cc}, T_m, ΔH_m, ΔH_{cc}) obtained from the first and second heating run are summarized in Tables 3 and 4, respectively. The crystallinity percentage (X_{cc}) of PLA and its composites is also reported. Furthermore, only the temperature of the second peak was reported as PLA melting temperature.

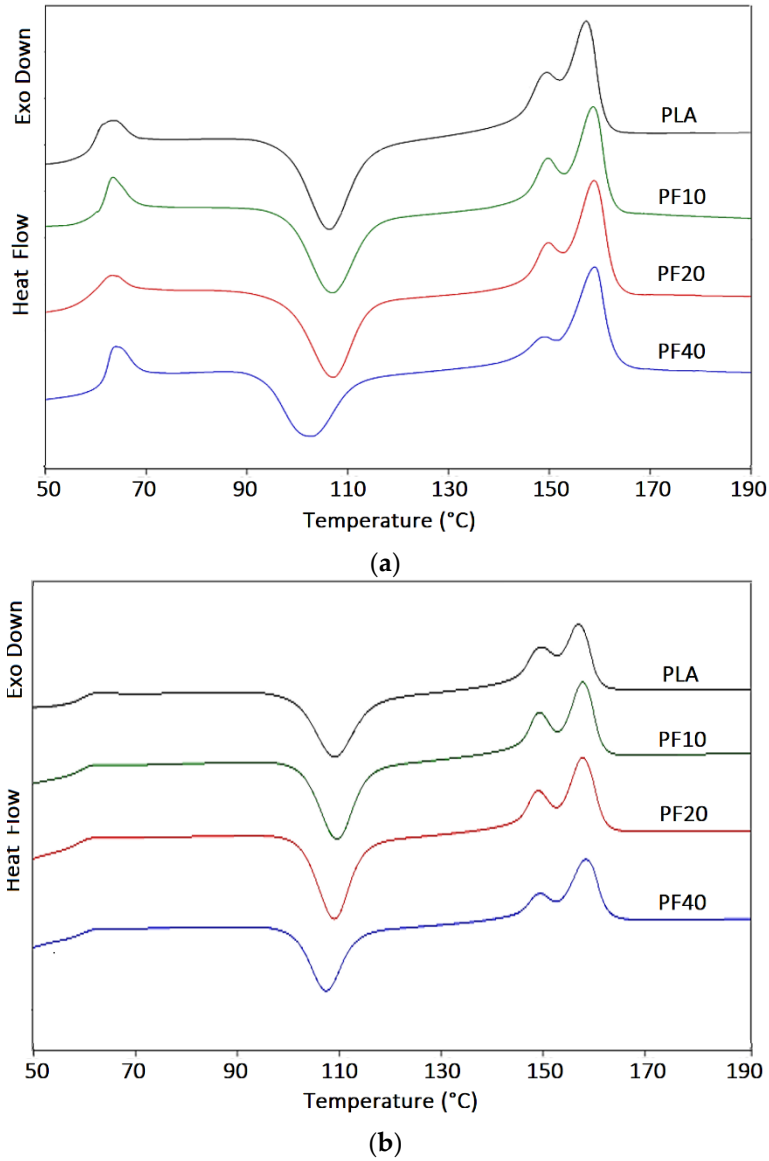

Figure 8. Differential scanning calorimetry (DSC) thermograms of neat PLA and its composites with flax fibers: (**a**) first and (**b**) second heating run.

Table 3. Thermal properties and crystallinity fraction (X_{cc}) of PLA and its composites (1st heating run).

PLA/Flax (wt./wt.%)	T_g (°C)	T_{cc} (°C)	T_m (°C)	ΔH_m (J/g)	ΔH_{cc} (J/g)	X_{cc} (%)
100/0	60.1	106.2	156.8	32.9	25.7	5.4
90/10	61.1	106.6	158.2	31.1	22.7	6.9
80/20	61.0	106.7	158.4	31.8	22.9	8.3
60/40	61.3	102.5	158.6	28.9	20.8	10.1

Table 4. Thermal properties and crystallinity fraction (X_{cc}) of PLA and its composites (2nd heating run).

PLA/Flax (wt./wt.%)	T_g (°C)	T_{cc} (°C)	T_m (°C)	ΔH_m (J/g)	ΔH_{cc} (J/g)	X_{cc} (%)
100/0	60.1	108.8	156.4	32.0	28.6	2.7
90/10	60.9	109.3	157.2	33.0	25.8	6.4
80/20	60.5	108.8	157.2	34.7	26.6	8.1
60/40	60.2	107.3	157.8	30.2	21.5	11.6

As shown, in the first heating, the glass transition of amorphous PLA, which typically occurs at 60 °C, is overlapped with an enthalpy recovery peak, due to permanence of the samples at room temperature before the tests. This effect disappeared in the second heating having deleted eliminated the sample thermal history.

The crystallinity slightly increased with the flax fiber content and at 40 wt.% fibers the crystallinity of PLA increased more than three times compared to pure PLA. A further trend that can be observed is the shifting of the cold crystallization peak to lower temperatures with the flax fiber amount. Consequently, the stiffness increment of the composites (Figure 2) with the increasing amount of fibers was due not only to the fiber stiffness but also to the PLA crystallinity increment.

The results of the DMTA, showed in Figure 9, confirm the nucleating effect of the flax fibers for the crystallization of PLA [52,53]. Both neat PLA and the composites start to soften after 60 °C (where the glass transition occurs); however, the decay of the elastic modulus is less marked for the composite with 40 wt.% of flax fibers. This result is in agreement with the DSC results in which the major crystallinity content is registered for this composite. More crystalline the polymer is, less marked is its elastic modulus decay near the T_g.

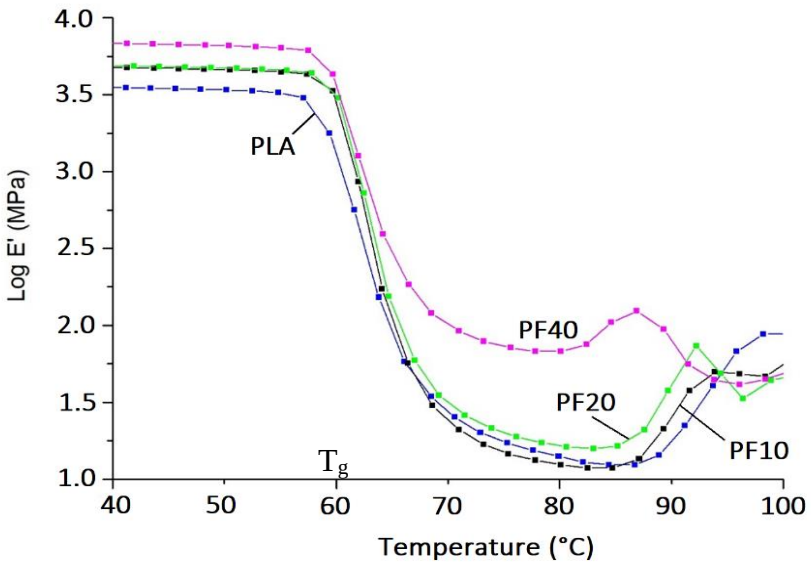

Figure 9. Dynamic modulus for PLA and PLA/flax fiber composites.

5. Conclusions

In this study PLA/short flax fiber composites with different content of fibers (10–40 wt.%) were produced by extrusion and characterized in terms of thermal, morphological, mechanical, and thermo-mechanical properties.

The flax fibers were not subjected to any superficial treatment in order to evaluate their intrinsic adhesion with the PLA matrix.

The processing of the composites by extrusion and injection molding, up to 40 wt.% of flax fiber content, did not create any difficulty. Consequently, they can be produced and processed using conventional melt processes and this is very important from the application point of view.

Although interfacial adhesion between natural fibers and polymeric matrices is generally weak, untreated flax fibers showed a good adhesion to the PLA matrix as confirmed by SEM images and also by the calculated Pukánszky's interaction B parameter (about 3.2) and the good fitting of the Einstein model to the experimental data for the prediction of Young modulus.

The well-known problem of PLA related to the low glass transition temperature was improved with the addition of significant amounts of flax fibers. In fact, short flax fibers acted both as reinforcement and nucleating agent for PLA, as confirmed by the mechanical and thermo-mechanical tests. The maximum value of stress at break (66 MPa) was obtained at 20 wt.% fibers and at 40 wt.% fibers an improvement in the elastic modulus decay near the glass transition temperature (60 °C) was observed.

Author Contributions: A.L. and M.S. supervised the study results and discussion; L.A. performed the experimental tests and modeling of the mechanical properties; L.A., V.G., and M.S. wrote the original draft; M.-B.C. and P.C. co-supervised the experimental activities.

Funding: This research received no external funding.

Acknowledgments: The authors acknowledge Luigi Torre of Perugia University that kindly provided the flax fibers.

Conflicts of Interest: The authors declare no conflict of interest.

References

1. Le Duigou, A.; Pillin, I.; Bourmaud, A.; Davies, P.; Baley, C. Effect of recycling on mechanical behaviour of biocompostable flax/poly(l-lactide) composites. *Compos. Part A Appl. Sci. Manuf.* **2008**, *39*, 1471–1478. [CrossRef]
2. Assarar, M.; Scida, D.; El Mahi, A.; Poilâne, C.; Ayad, R. Influence of water ageing on mechanical properties and damage events of two reinforced composite materials: Flax–fibres and glass–fibres. *Mater. Des.* **2011**, *32*, 788–795. [CrossRef]
3. Ibrahim, N.A.; Yunus, W.M.Z.W.; Othman, M.; Abdan, K.; Hadithon, K.A. Poly(Lactic Acid) (PLA)-reinforced kenaf bast fiber composites: The effect of triacetin. *J. Reinf. Plast. Compos.* **2010**, *29*, 1099–1111. [CrossRef]
4. Gurunathan, T.; Mohanty, S.; Nayak, S.K. A review of the recent developments in biocomposites based on natural fibres and their application perspectives. *Compos. Part A Appl. Sci. Manuf.* **2015**, *77*, 1–25. [CrossRef]
5. Bos, H.L.; Müssig, J.; Oever, M.J.V.D. Mechanical properties of short-flax-fibre reinforced compounds. *Compos. Part A Appl. Sci. Manuf.* **2006**, *37*, 1591–1604. [CrossRef]
6. Aliotta, L.; Gigante, V.; Coltelli, M.B.; Cinelli, P.; Lazzeri, A. Evaluation of Mechanical and Interfacial Properties of Bio-Composites Based on Poly(Lactic Acid) with Natural Cellulose Fibers. *Int. J. Mol. Sci.* **2019**, *20*, 960. [CrossRef] [PubMed]
7. Righetti, M.C.; Cinelli, P.; Mallegni, N.; Massa, C.A.; Aliotta, L.; Lazzeri, A. Properties of Poly (lactic acid) based Biocomposites with Potato Pulp Powder Treated with Waxes. *Materials* **2019**, *12*, 990. [CrossRef] [PubMed]
8. Bledzki, A. Composites reinforced with cellulose based fibres. *Prog. Polym. Sci.* **1999**, *24*, 221–274. [CrossRef]
9. Mohanty, A.K.; Misra, M.; Hinrichsen, G. Biofibres, biodegradable polymers and biocomposites: An overview. *Macromol. Mater. Eng.* **2000**, *276*, 1–24. [CrossRef]
10. Bos, H.L.; Oever, M.J.A.V.D.; Peters, O.C.J.J. Tensile and compressive properties of flax fibres for natural fibre reinforced composites. *J. Mater. Sci.* **2002**, *37*, 1683–1692. [CrossRef]

11. Ahmed, S.; Ulven, C.A. Dynamic In-Situ Observation on the Failure Mechanism of Flax Fiber through Scanning Electron Microscopy. *Fibers* **2018**, *6*, 17. [CrossRef]
12. Thuault, A.; Domengès, B.; Hervás, I.; Gomina, M. Investigation of the internal structure of flax fibre cell walls by transmission electron microscopy. *Cellulose* **2015**, *22*, 3521–3530. [CrossRef]
13. Cinelli, P.; Mallegni, N.; Gigante, V.; Montanari, A.; Seggiani, M.; Coltelli, B.; Bronco, S.; Lazzeri, A. Biocomposites Based on Polyhydroxyalkanoates and Natural Fibres from Renewable Byproducts. *Appl. Food Biotechnol.* **2019**, *6*, 35–43.
14. Seggiani, M.; Cinelli, P.; Balestri, E.; Mallegni, N.; Stefanelli, E.; Rossi, A.; Lardicci, C.; Lazzeri, A. Novel Sustainable Composites Based on Poly(hydroxybutyrate-co-hydroxyvalerate) and Seagrass Beach-CAST Fibers: Performance and Degradability in Marine Environments. *Materials* **2018**, *11*, 772. [CrossRef] [PubMed]
15. Seggiani, M.; Cinelli, P.; Mallegni, N.; Balestri, E.; Puccini, M.; Vitolo, S.; Lardicci, C.; Lazzeri, A. New Bio-Composites Based on Polyhydroxyalkanoates and Posidonia oceanica Fibres for Applications in a Marine Environment. *Materials* **2017**, *10*, 326. [CrossRef]
16. Raquez, J.-M.; Habibi, Y.; Murariu, M.; Dubois, P. Polylactide (PLA)-based nanocomposites. *Prog. Polym. Sci.* **2013**, *38*, 1504–1542. [CrossRef]
17. Aliotta, L.; Cinelli, P.; Coltelli, M.B.; Righetti, M.C.; Gazzano, M.; Lazzeri, A. Effect of nucleating agents on crystallinity and properties of poly (lactic acid) (PLA). *Eur. Polym. J.* **2017**, *93*, 822–832. [CrossRef]
18. Gigante, V.; Canesi, I.; Cinelli, P.; Coltelli, M.B.; Lazzeri, A. Rubber Toughening of Polylactic Acid (PLA) with Poly(butylene adipate-co-terephthalate) (PBAT): Mechanical Properties, Fracture Mechanics and Analysis of Ductile-to-Brittle Behavior while Varying Temperature and Test Speed. *Eur. Polym. J.* **2019**, *115*, 125–137. [CrossRef]
19. Aliotta, L.; Cinelli, P.; Beatrice Coltelli, M.; Lazzeri, A. Rigid filler toughening in PLA-Calcium Carbonate composites: Effect of particle surface treatment and matrix plasticization. *Eur. Polym. J.* **2018**. [CrossRef]
20. Argon, A.; Cohen, R. Toughenability of polymers. *Polymer* **2003**, *44*, 6013–6032. [CrossRef]
21. Byun, Y.; Rodríguez, K.; Han, J.H.; Kim, Y.T. Improved thermal stability of polylactic acid (PLA) composite film via PLA–β-cyclodextrin-inclusion complex systems. *Int. J. Boil. Macromol.* **2015**, *81*, 591–598. [CrossRef] [PubMed]
22. Thakur, V.K.; Thakur, M.K.; Gupta, R.K. Review: Raw Natural Fiber–Based Polymer Composites. *Int. J. Polym. Anal. Charact.* **2014**, *19*, 256–271. [CrossRef]
23. Dittenber, D.B.; GangaRao, H.V. Critical review of recent publications on use of natural composites in infrastructure. *Compos. Part A Appl. Sci. Manuf.* **2012**, *43*, 1419–1429. [CrossRef]
24. Jawaid, M.; Khalil, H.A. Cellulosic/synthetic fibre reinforced polymer hybrid composites: A review. *Carbohydr. Polym.* **2011**, *86*, 1–18. [CrossRef]
25. Biagiotti, J.; Puglia, D.; Torre, L.; Arbelaiz, A.; Cantero, G.; Marieta, C.; Llano-Ponte, R. A systematic investigation on the influence of the chemical treatment of natural fibers on the properties of their polymer matrix composites. *Polym. Compos.* **2004**, *25*, 470–479. [CrossRef]
26. Baley, C.; Busnel, F.; Grohens, Y.; Sire, O. Influence of chemical treatments on surface properties and adhesion of flax fibre–polyester resin. *Compos. Part A Appl. Sci. Manuf.* **2006**, *37*, 1626–1637. [CrossRef]
27. Arbelaiz, A.; Cantero, G.; Fernandez, B.; Mondragon, I.; Gañán, P.; Kenny, J.M. Flax fiber surface modifications: Effects on fiber physico mechanical and flax/polypropylene interface properties. *Polym. Compos.* **2005**, *26*, 324–332. [CrossRef]
28. Sawpan, M.A.; Pickering, K.L.; Fernyhough, A. Effect of fibre treatments on interfacial shear strength of hemp fibre reinforced polylactide and unsaturated polyester composites. *Compos. Part A Appl. Sci. Manuf.* **2011**, *42*, 1189–1196. [CrossRef]
29. Graupner, N.; Rößler, J.; Ziegmann, G.; Müssig, J. Fibre/matrix adhesion of cellulose fibres in PLA, PP and MAPP: A critical review of pull-out test, microbond test and single fibre fragmentation test results. *Compos. Part A Appl. Sci. Manuf.* **2014**, *63*, 133–148. [CrossRef]
30. Oksman, K.; Skrifvars, M.O.V.; Selin, J.-F. Natural fibres as reinforcement in polylactic acid (PLA) composites. *Compos. Sci. Technol.* **2003**, *63*, 1317–1324. [CrossRef]
31. Bax, B.; Müssig, J. Impact and tensile properties of PLA/Cordenka and PLA/flax composites. *Compos. Sci. Technol.* **2008**, *68*, 1601–1607. [CrossRef]

32. Zhang, J.; Duan, Y.; Sato, H.; Tsuji, H.; Noda, I.; Yan, S.; Ozaki, Y. Crystal Modifications and Thermal Behavior of Poly (L -lactic acid) Revealed by Infrared Spectroscopy. *Macromolecules* **2005**, *38*, 8012–8021. [CrossRef]
33. Righetti, M.C.; Gazzano, M.; Di Lorenzo, M.L.; Androsch, R. Enthalpy of melting of α′- and α-crystals of poly(l-lactic acid). *Eur. Polym. J.* **2015**, *70*, 215–220. [CrossRef]
34. Renner, K.; Kenyó, C.; Móczó, J.; Pukánszky, B. Micromechanical deformation processes in PP/wood composites: Particle characteristics, adhesion, mechanisms. *Compos. Part A Appl. Sci. Manuf.* **2010**, *41*, 1653–1661. [CrossRef]
35. Kelly, A.; Tyson, W. Tensile properties of fibre-reinforced metals: Copper/tungsten and copper/molybdenum. *J. Mech. Phys. Solids* **1965**, *13*, 329–350. [CrossRef]
36. Piggott, M.R. Short Fibre Polymer Composites: A Fracture-Based Theory of Fibre Reinforcement. *J. Compos. Mater.* **1994**, *28*, 588–606. [CrossRef]
37. Bader, M.; Bowyer, W. An improved method of production for high strength fibre-reinforced thermoplastics. *Composites* **1973**, *4*, 150–156. [CrossRef]
38. Pukánszky, B. Influence of interface interaction on the ultimate tensile properties of polymer composites. *Composites* **1990**, *21*, 255–262. [CrossRef]
39. Turcsányi, B.; Pukánszky, B.; Tüdös, F. Composition dependence of tensile yield stress in filled polymers. *J. Mater. Sci. Lett.* **1988**, *7*, 160–162. [CrossRef]
40. Kim, H.G.; Kwac, L.K. Evaluation of elastic modulus for unidirectionally aligned short fiber composites. *J. Mech. Sci. Technol.* **2009**, *23*, 54–63. [CrossRef]
41. Fu, S.-Y.; Feng, X.-Q.; Lauke, B.; Mai, Y.-W. Effects of particle size, particle/matrix interface adhesion and particle loading on mechanical properties of particulate–polymer composites. *Compos. Part B Eng.* **2008**, *39*, 933–961. [CrossRef]
42. Bourkas, G.; Prassianakis, I.; Kytopoulos, V.; Sideridis, E.; Younis, C. Estimation of Elastic Moduli of Particulate Composites by New Models and Comparison with Moduli Measured by Tension, Dynamic, and Ultrasonic Tests. *Adv. Mater. Sci. Eng.* **2010**, *2010*, 1–13. [CrossRef]
43. Einstein, A.; Fürth, R. *Investigations on the Theory of Brownian Movement*; Dover Publications: New York, NY, USA, 1956.
44. Affdl, J.C.H.; Kardos, J.L. The Halpin-Tsai equations: A review. *Polym. Eng. Sci.* **1976**, *16*, 344–352. [CrossRef]
45. Cox, H.L. The elasticity and strength of paper and other fibrous materials. *Br. J. Appl. Phys.* **1952**, *3*, 72–79. [CrossRef]
46. Fu, S.-Y. Effects of fiber length and fiber orientation distributions on the tensile strength of short-fiber-reinforced polymers. *Compos. Sci. Technol.* **1996**, *56*, 1179–1190. [CrossRef]
47. Zhu, J.; Zhu, H.; Njuguna, J.; Abhyankar, H. Recent Development of Flax Fibres and Their Reinforced Composites Based on Different Polymeric Matrices. *Materials* **2013**, *6*, 5171–5198. [CrossRef] [PubMed]
48. Yan, L.; Chouw, N.; Jayaraman, K. Flax fibre and its composites—A review. *Compos. Part B Eng.* **2014**, *56*, 296–317. [CrossRef]
49. Martin, N.; Mouret, N.; Davies, P.; Baley, C. Influence of the degree of retting of flax fibers on the tensile properties of single fibers and short fiber/polypropylene composites. *Ind. Crop. Prod.* **2013**, *49*, 755–767. [CrossRef]
50. Van De Weyenberg, I.; Truong, T.C.; Vangrimde, B.; Verpoest, I. Improving the properties of UD flax fibre reinforced composites by applying an alkaline fibre treatment. *Compos. Part A Appl. Sci. Manuf.* **2006**, *37*, 1368–1376. [CrossRef]
51. Heinemann, M.; Fritz, H.G. Polylactid-Struktur, Eigenschaften and Anwendungen. In *Stuttgarter Kunststoff-Kolloquium, 19*; Universität Stuttgart: Stuttgart, Germany, 2005.
52. Kumar, R.; Nair, K.; Thomas, S.; Schit, S.; Ramamurthy, K. Morphology and melt rheological behaviour of short-sisal-fibre-reinforced SBR composites. *Compos. Sci. Technol.* **2000**, *60*, 1737–1751. [CrossRef]
53. Yu, L.; Dean, K.; Li, L. Polymer blends and composites from renewable resources. *Prog. Polym. Sci.* **2006**, *31*, 576–602. [CrossRef]